From Regioirregular Linear Main-Chain Liquid-Crystal Polyethers Exhibiting Two Uniaxial Nematic Phases to Macrocyclic Main-Chain Oligoethers Displaying Nematic and Smectic Phases

V. Percec* and A. D. Asandei

The W. M. Keck Laboratories for Organic Synthesis, Department of Macromolecular Science, Case Western Reserve University, Cleveland, Ohio 44106-7202

G. Ungar

Department of Engineering Materials and Center for Molecular Materials, The University of Sheffield, Sheffield, S1 4DU, UK

Received March 26, 1996[⊗]

The synthesis and characterization of regioirregular macrocyclics based on the conformationally flexible 1-(4-hydroxyphenyl)-2-(2-methyl-4-hydroxyphenyl)ethane (MBPE) and α,ω-dibromoalkanes, *i.e.*, MBPE-(c)*X*(z) (where c stands for cyclic, $X = 4$, 5, 9, and 11 represents the number of methylenic groups in the flexible spacer and $z = 1-5$ is the degree of oligomerization of the macrocyclic) and the comparison of their phase behavior with that of the corresponding high molecular weight linear polymers MBPE-(l)X (where l stands for linear and X has the same meaning as in the case of cyclics) are described. The effects of *X* and *z* on the phase behavior of MBPE-(c)*X*(*z*) is discussed. For proper (*X*, *z*) pairs such as (4, 5), (5, 4), (9, 3), (9, 4), (11, 3), and (11, 4), MBPE-(c)X(z) have a higher ability to generate and stabilize liquid-crystalline (LC) phases than the corresponding linear polymers. MBPE-(l)*X* with $X =$ odd numbers exhibit two uniaxial nematic phases. MBPE-(c)*X*(*z*) do not display the second uniaxial nematic phase that is exhibited by the linear polymers. This second nematic phase is converted to a smectic A phase through cyclization. An explanation for this behavior is suggested.

Introduction

The first examples of macrocyclic main-chain liquid crystals (LC) were reported from our laboratory in 1992.[1] Simultaneous with this discovery we demonstrated that macrocyclic compounds display a higher ability to form LC phases than the corresponding linear homologues (Scheme 1).[1,2] Therefore the *cyclic* and not the *linear* shape provides the optimum architecture that yields liquid crystallinity. Macrocyclic LCs based on conformationally flexible mesogens and flexible spacers exhibit uniaxial nematic,[1,2] smectic A,[2] and biaxial nematic[5] mesophases which are obtained from their quasi-rod-like collapsed conformation. This collapsed conformation is more rigid than the corresponding linear one.[4] Similarities and differences between main chain linear and macrocyclic compounds were discussed.[2b,f,5]

Scheme 1. Dependence of the Isotropization Temperature of Cyclic and Linear Main-Chain LC Polymers on the Degree of Polymerization (Both Ti and DP in Arbitrary Units)

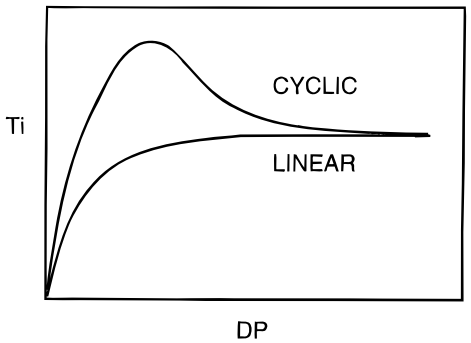

Our efforts are directed toward the elaboration of simple synthetic methods to produce cyclic compounds in large quantities[6], preparation of polymers based on macrocyclic compounds,[7] and of other LC with more complex architecture based on macrocyclic building blocks. Simultaneously, we are concerned with the elucidation of the influence of the molecular architecture on the structure of the mesophase formed.

In a series of publications from our laboratory we reported the discovery of two uniaxial nematic meso-

[⊗] Abstract published in *Advance ACS Abstracts,* July 1, 1996.

(1) Percec, V.; Kawasumi, M.; Rinaldi, P. M.; Litman, V. E. *Macromolecules* **1992**, *25*, 3851.

(2) (a)Percec, V.; Kawasumi, M. *Adv. Mater.* **1992**, *4*, 572. (b) Percec, V.; Kawasumi, M. *Macromolecules* **1993**, *26*, 3663. (c) Percec, V.; Kawasumi, M. *Macromolecules* **1993**, *26*, 3917. (d) Percec, V.; Kawasumi, M. *Liq. Cryst.* **1993**, *13*, 83. (e) Percec, V.; Kawasumi, M. *Chem. Mater.* **1993**, *5*, 826. (f) Percec, V.; Kawasumi, M. *J. Mater. Chem.* **1993**, *3*, 725. (g) Percec, V.; Kawasumi, M. *Mol. Cryst. Liq. Cryst.* **1994**, *238*, 21. (h) Percec, V.; Kawasumi, M. *J. Chem. Soc., Perkin Trans. 1* **1993**, 1319.

(3) (a) Li, J. F.; Percec, V.; Rosenblatt, C. *Phys. Rev. E* **1993**, *48*, R1. (b) Li, J. F.; Percec, V.; Rosenblatt, C.; Lavrentovich, O. D. *Europhys. Lett.* **1994**, *25*, 199.

(4) Chen, F. L.; Jamieson, A. M.; Kawasumi, M.; Percec, V. *J. Polym. Sci., Part B: Polym. Phys.* **1995**, *33*, 1213.

(5) Percec, V. *Pure Appl. Chem.* **1995**, *67*, 2031.

(6) Percec, V.; Asandei, A. D.; Zhao, M. *Chem. Mater.* **1996**, *8*, 301.

(7) Percec, V.; Asandei, A. D.; Chu, P. *Macromolecules* **1996**, *29*, 3736.

S0897-4756(96)00204-9 CCC: $12.00

Scheme 2. Synthesis of Cyclic Polyethers Based on MBPE and α,ω-Dibromoalkanes Containing *X* = 4, 5, 9, and 11 Methylenic Units

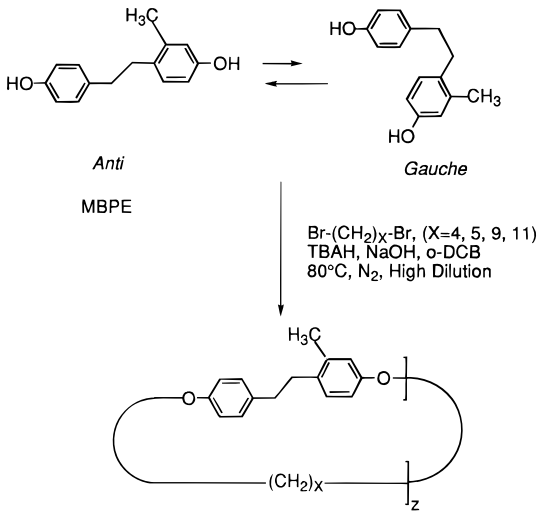

phases in linear main chain LCPs[8] based on 1-(4-hydroxyphenyl-2-(2-R-4-hydroxy)ethane (RBPE where R = CH_3, CF_3, Cl, Br, F) and odd flexible spacers. Recently, these two uniaxial nematic mesophases were explained theoretically.[9]

The goal of this publication is to report the synthesis of cyclic regioirregular main-chain liquid-crystalline oligoethers based on 1-(4-hydroxyphenyl)-2-(2-methyl-4-hydroxyphenyl)ethane (MBPE) and flexible spacers containing 4, 5, 9, and 11 methylenic units, *i.e.*, MBPE-(c)*X*(*z*) (where c stands for cyclic, *X* represents the number of methylenic groups in the flexible spacer, and *z* = degree of oligomerization of the macrocyclic). The corresponding regioirregular linear polyethers based on MBPE and flexible spacers, *i.e.*, MBPE-(l)*X* containing an odd number of methylenic units display two uniaxial nematic mesophases.[8] These experiments will demonstrate that the two uniaxial nematic mesophases are not obtained in macrocyclic compounds. In several cases, such as MBPE-(c)4(4), MBPE-(c)5(4), MBPE-(c)9-(3), MBPE-(c)9(4), MBPE-(c)11(3), and MBPE-(c)11(4), the cyclic compound exhibits a uniaxial nematic phase and a smectic A phase. These results support the theoretical explanation provided by Luckhurst et al.[9] on the mechanism of formation of two uniaxial nematic phases.

Experimental Section

Materials. Tetrabutylammonium hydrogen sulfate (TBAH, 97%, Aldrich) was used as received. 1,4-Dibromobutane, 1,5-dibromopentane, 1,9-dibromononane, 1,11-dibromoundecane, and *o*-dichlorobenzene (*o*-DCB; all from Aldrich) were purified by vacuum distillation. 1-(4-Hydroxyphenyl)-2-(2-methyl-4-hydroxyphenyl)ethane (MBPE, purity >99%, HPLC), was synthesized as previously described.[8g] SiO_2 thin-layer chromatography plates with fluorescent indicator (Kodak) and all other commercially available chemicals were used as received.

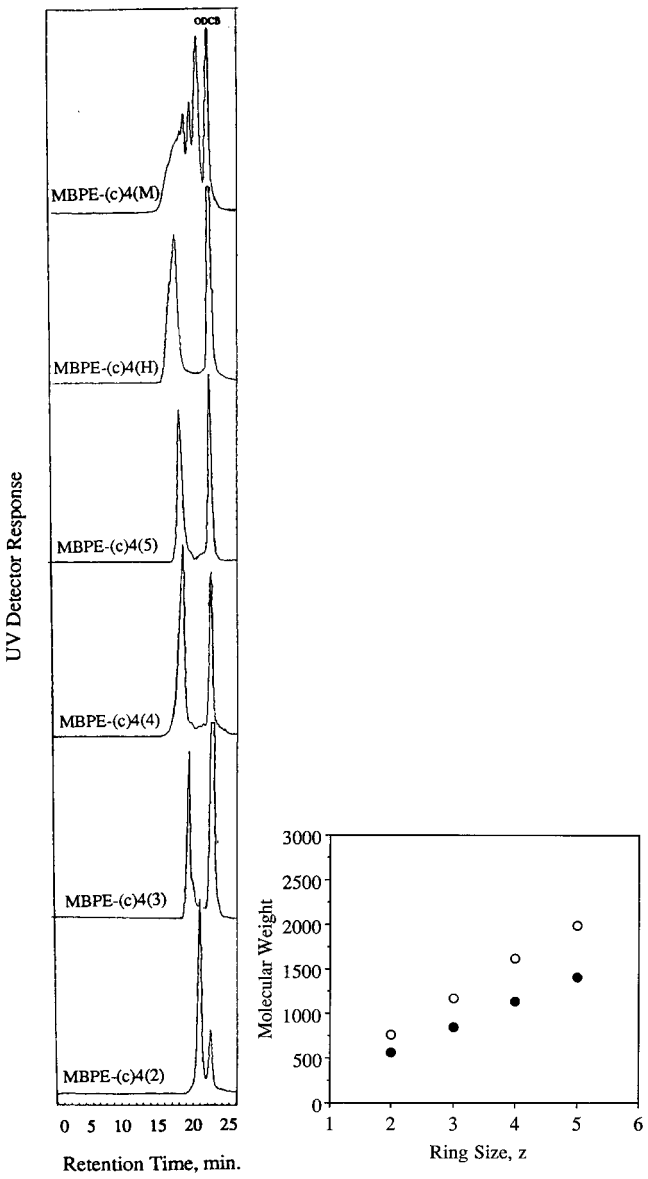

Figure 1. (a, left) GPC chromatograms of the cyclization mixture (MBPE-(c)4(M)), of the higher molecular weight part (MBPE-(c)4(H)), and of the separated cyclic oligomers of the MBPE-(c)4(*z*) (*z* = 2−5) series. (b, right) Corresponding dependence of the theoretical (●) and experimental (○) molecular weights of the MBPE-(c)4(*z*) on ring size.

Synthesis of Macrocyclic Polyethers MBPE-(c)*X*(*z*) (*X* = 4, 5, 9, and 11). The MBPE-(c)*X*(*z*) macrocyclics were synthesized by the phase-transfer-catalyzed polyetherification of MBPE with the corresponding α,ω-dibromoalkanes under high dilution conditions, under a N_2 atmosphere, in a two-phase (*o*-DCB/aqueous NaOH) system, using TBAH as phase-transfer catalyst. An example is as follows: A mixture of MBPE (0.68 g, 3 mmol), 1,9-dibromononane (0.85.g, 3 mmol), TBAH (0.41 g, 1.2 mmol), o-DCB (300 mL), and NaOH (300 mL, 10 N) was stirred vigurously at 80 °C under N_2. After 40 h the reaction mixture was diluted with water and chloroform. The organic layer was washed with water, dilute HCl, and water. The solvent was distilled, and the resulting solid mixture (MBPE-(c)9(M)) was charged on a SiO_2 packed column. The mixture of low molecular weight macrocyclics (MPPE-(c)9(*z*), *z* = 1−4) was separated from the mixture of higher molecular weight linear and cyclic compounds (MBPE-(c)9(H)) by elution with acetone. MBPE-(c)9(H) was eluted with $CHCl_3$. Individual macrocyclics were isolated by column chromatography (SiO_2, acetone/hexane = 1/30 (v/v)).

(8) (a) Percec, V.; Tsuda, Y. *Macromolecules* **1990**, *23*, 5. (b) Percec, V.; Tsuda, Y. *Macromolecules* **1990**, *23*, 3509. (c) Ungar, G.; Percec, V.; Zuber, M. *Macromolecules* **1992**, *25*, 75. (d) Ungar, G.; Percec, V.; Zuber, M. *Polym. Bull.* **1994**, *32*, 325. (e) Silvestri, R. L.; Koenig, J. L. *Polymer* **1994**, *35*, 2528. (f) Ungar, G.; Zhou, J.; Percec, V.; Chu, P. *Macromol. Symp.* **1995**, *98*, 951. (g) Percec, V.; Yourd, R. *Macromolecules* **1989**, *22*, 524.

(9) (a) Ferrarini, A.; Luckhurst, G. R.; Nordio, P. L.; Roskilly, S. J. *Chem. Phys. Lett.* **1993**. *214*, 409. (b) Luckhurst, G. R. *Macromol. Symp.* **1995**, *96*, 1.

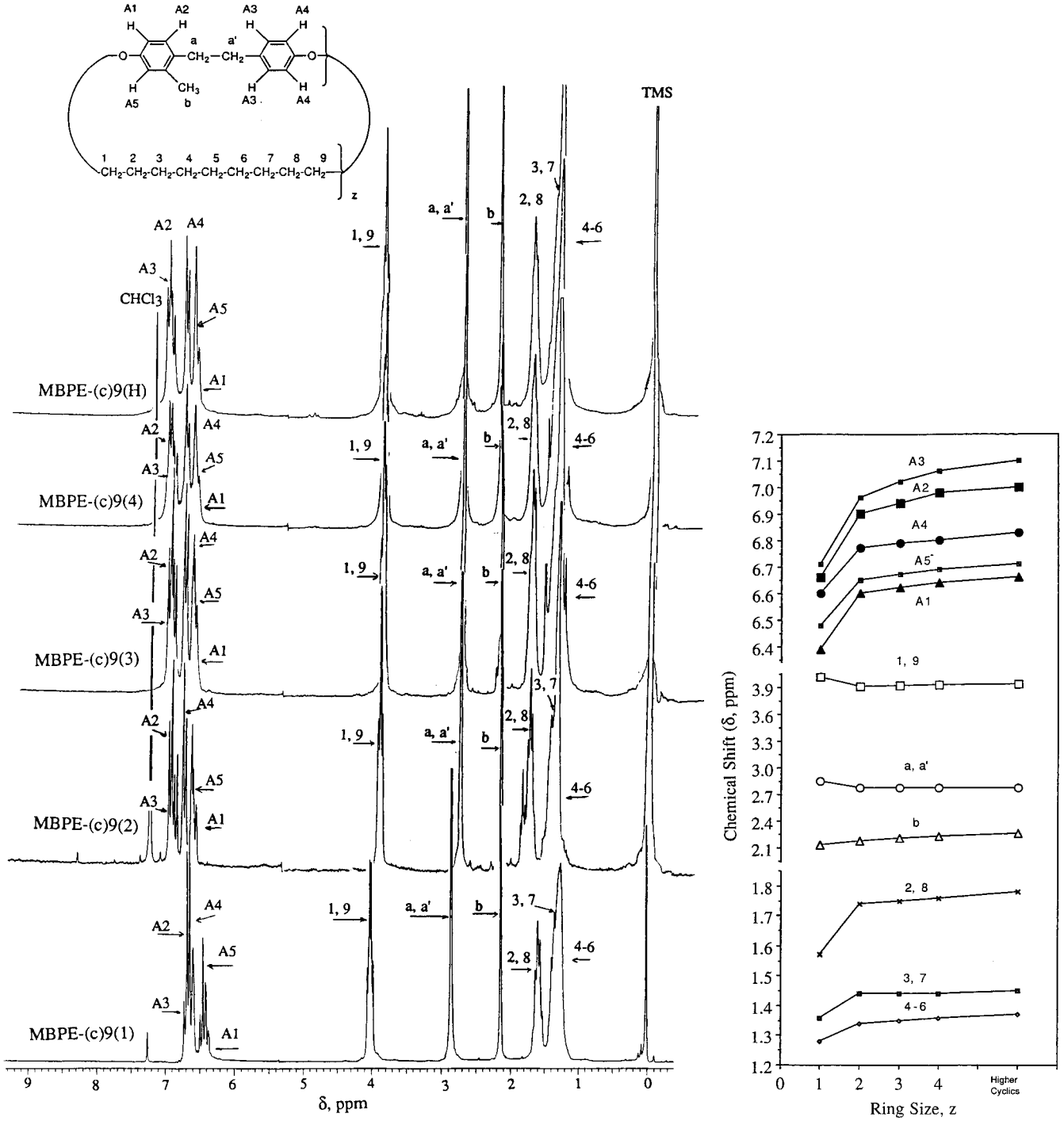

Figure 2. (a, left) The 200 MHz ^{1}H MNR spectra ($CDCl_3$, TMS) of the MBPE-(c)9(*z*) (*z* = 1−4) series and of the mixture of higher oligomers. (b, right) Corresponding dependence of the chemical shifts on ring size.

Techniques. A 200 MHz Varian Gemini 200 spectrometer was used to record the ^{1}H-NMR spectra at 20 °C. TMS was used as internal standard. The purity of the products was determined by a combination of thin-layer chromaography (TLC) on silica gel plates with fluorescent indicator and high-pressure liquid chromatography (HPLC) using a Perkin-Elmer Series 10LC high-pressure liquid chromatograph, equipped with an LC-100 column oven, Nelson Analytical 900 Series data station, and a UV detector (detection at 254 nm). The measurements were done using THF as solvent (1 mL/min, 40 °C) and two PL gel columns of 5×10^2 and 10^4 Å. Relative molecular weights were determined with the same instrument by using a calibration plot constructed with polystyrene standards. A Perkin-Elmer PC Series DSC-7 differential scanning calorimeter equipped with a TAC7/DX thermal analysis controller was used to record the first-order thermal transitions which were read at the maximum or minimum of the endothermic or exothermic peaks. Glass transitions (*Tg*) were measured at the middle point of the change in heat capacity. The instrument was calibrated with In and Zn standards. Scanning rates were 20 °C/min in all cases. All heating and cooling scans were perfectly reproducible after the first heating scan. The first heating scan could be reobtained after proper annealing. An Olympus BX40 optical polarizing microscope equipped with a Mettler FP 82 hot stage and a Mettler FP 800 central processor was used to analyze the anisotropic textures. X-ray scattering patterns were recorded by using either a helium-filled, flat plate, wide-angle (WAXS) camera or a pinhole-collimated small-angle (SAXS) camera and an image plate area detector (MAR Research) with a graphite-monochromatized pinhole-collimated beam and a helium tent. The samples, in glass capillaries, were held in a temperature-controlled cell (±0.1 °C). Ni-filtered Cu Kα radiation was used. Molecular modeling was performed on a Silicon Graphics

Table 1. Characterization of MBPE-(c)*X*(*z*) (Data from the Corresponding MBPE-(l)*X*[8b] Also Included)

macrocycle and linear polymer	separated yield (%)	purity (HPLC) (%)	molecular wt theoretical	molecular wt experimental (GPC)	transitions temp (°C) (corresponding enthalpy changes (Kcal/mru)[a] first and second heating	transitions temp (°C) (corresponding enthalpy changes (Kcal/mru)[a] first cooling
MBPE-(c)4(2)	8.6	98.7	564	764	k 123 (0.3) k 158 (6.4) i k158 (6.06) i	i 115 (5.45) k
MBPE-(c)4(3)	4.3	96.2	846	1170	k 75 i g 15 i	i 6 g
MBPE-(c)4(4)	1.1	94.4	1128	1622	g 20 k 61 (−2.9) k 85 (1.54) k 142 (6.41) i g 20 k 61 (−2.9) k 85 (1.54) k 142 (6.41) i	i 92 n (0.27) s_A 31 (0.18) 10 g
MBPE-(c)4(5)	0.7	93.6	1410	1994	k 53 (0.53) k 80 (0.12) k 101 (0.94) g 16 n 79 (0.31) i	i 70 (0.28) n 9 g
MBPE-(c)4(H)	18.3			2.8×10^3	k 127 (1.5) k 141 (1.02) k 163 (1.34) i k 135 (0.83) k 155 (1.89) k 164 (0.92) i	i 127 (3.64) k
MBPE-(l)4				4.1×10^3	k 51 (0.06) k 187 (5.04) i k 171 k 187 (5.53) i	i 160 (4.90) k
MBPE-(c)5(2)	5.4	97.3	592	670	k 6 (1.48) k 50 (7.4) k 131 (3.99) i k 50 (−2.52) k 131 (3.99) i	i
MBPE-(c)5(3)	2.8	92.1	888	1005	k 30 i g 8 i	i 3 g
MBPE-(c)5(4)	1.5	96.7	1184	1360	k 118 (4.74) i g 18 s_A 31 (0.06) n 50 (0.02)i	i 43 (0.02) n 23 (0.06) s_A 8 g
MBPE-(c)5(H)	25.8			5×10^3	k 50 (0.37) k 84 (2.4) k 100 (0.44) i g 15 k 48 k 87 (0.66) k 100 (0.45) i	i 55 (0.32) n 41 (0.25) 10 g
MBPE-(l)5				1.9×10^4	k 44 (0.25) k 119 (3.47) g 20 k 79 (1.44) k 115 (0.33) i	i 51 (0.57) n_1 37 (0.10) n2 13 g
MBPE-(c)9(1)	7.1	96.8	352	400	i i	i
MBPE-(c)9(2)	6.2	98.7	704	811	k 103 (5.67) k 113 (1.89) i k 85 (−0.62) k 103 (6.47) k 117 (0.32) i	i 66 (6.47) k
MBPE-(c)9(3)	2.5	95.2	1056	1303	k 55 i g −2 s_A 43 (0.34) n 50 (0.11) i	i 43 (0.11) n 36 (0.33) s_A −19 g
MBPE-(c)9(4)	1.4	94.6	1408	1612	k 35 k 60 (1.53) k 103 (1.52) i g −7 k 25 (−2.35) k 80(0.33) k 103 (2.77) i	i 78 (0.32) n 48 (0.10) s_A −13 g
MBPE-(c)9(H)				5.5×10^3	k 64 (0.83) k 81 (1.87) i g 5 k 19 (−0.78) k 64 (1.21) k 81 (1.87) i	i 68 (0.41) n 56 (0.88) k 21 (0.92) −3 g
MBPE-(l)9				2.1×10^4	k 46 (0.24) k 80 k 89 (3.89) i g 6 k 75 k 80 k 91 (4.02) i	i 69 (1.05) n_1 58 (0.06) n2 48 (2.13) k 0 g
MBPE-(c)11(1)	5.2	92.3	380	443	i i	i
MBPE-(c)11(2)	3.2	94.5	760	890	k 78 (0.20) k 111 (6.44) i k 78 (-0.13) k 110 (6.62) i	i 44 (0.23) k 23 (4.31)k
MBPE-(c)11(3)	2.1	92.4	1140	1140	k 52 i g −12 s_A 42 (0.39) n 50 (0.13) i	i 41 (0.14) n 34 (0.32) s_A −16 g
MBPE-(c)11(4)	1.1	91.2	1520	2277	k 45 (1.40) k 57 (3.05) k 81 (1.91) i k 32 k 48 (1.08) k 67 (1.54) k 81 (1.66) i	i 65 (0.41) n 8 (1.69) s_A
MBPE-(c)11(H)	24.3			7.1×10^3	k 40 (0.28) k 71 (1.73) k 86 (2.72) i k 30 k 72 (2.11) k 86 (3.05) i	i 64 (1.36) n 42 (3.17) k
MBPE-(l)11				2.9×10^4	k 44 (0.56) k 98 (4.50) i g 5 k 101 (5.21) i	i 72 (1.09) n 64 (2.66) k

[a] Data from the first heating and cooling are on the first line, those from the second heating on the second line.

computer using the MacroModel software (version 5, Columbia University) and the MM3 force field for energy minimization.

Results and Discussion

Scheme 2 outlines the synthesis of MBPE-(c)*X*(*z*). The MBPE mesogenic unit has two conformers which are in dynamic equilibrium in solution and in the isotropic melt. In the LC phase of the MBPE based main chain linear oligomers and polymers only the anti conformer exists.[8cd,10] In the LC phases of main-chain cyclic oligomers the ratio between the anti and gauche conformers is determined by the ring size *z*, and the relationship between the length of the spacer and that of the conformationally flexible mesogen.[2f,5] While the anti conformer stabilises the LC phase, the gauche conformer of MBPE favors the cyclization reaction. Phase-transfer catalyzed etherification of MBPE with an α,ω-dibromoalkane carried out under high dilution affords after separation by column chromatography up to five oligomeric macrocyclics and a mixture of higher cyclics. An example of the GPC traces of the reaction mixture, of the higher molecular weight fraction eluted with $CHCl_3$, and of the individual isolated macrocyclics is presented in Figure 1a. The dependences of the theoretical and experimental molecular weights of MBPE-(c)4(*z*) on ring size are ploted in Figure 1b. The experimental molecular weights of these macrocyclics are higher than the theoretical values since the hydrodynamic volume of the cyclics is, as expected, smaller than that of the linear polystyrene used for the calibration of the GPC. Nevertheless, the linear plot from Figure 1b demonstrates the expected linear dependence between the hydrodynamic volume and ring size and, therefore, the correct *z* values of these cyclic compounds.

Additional proof for the cyclic nature of these oligomers is provided by their 200 MHz ^{1}H NMR spectra. The assignments of these spectra was made in a manner analogous to those of the TPB-(c)*X*(*z*) series.[1] Figure 2a shows the 200 MHz ^{1}H NMR spectra of MBPE-(c)9-(*z*), while Figure 2b plots the dependence of the corresponding chemical shifts on *z*. Two significant features of these spectra are used to ascertain the cyclic structure

(10) (a) Leissen, J.; Boeffel, C.; Spiess, H. W.; Yoon, D. Y.; Sherwood, M. H.; Kawasumi, M.; Percec, V. *Macromolecules* **1995**, *28*, 6937. (b) Hardouin, F.; Sigaud, G.; Archard, M. F.; Brûlet, A.; Cotton, P. J.; Yoon, D. Y.; Percec, V.; Kawasumi, M. *Macromolecules* **1995**, *28*, 5427.

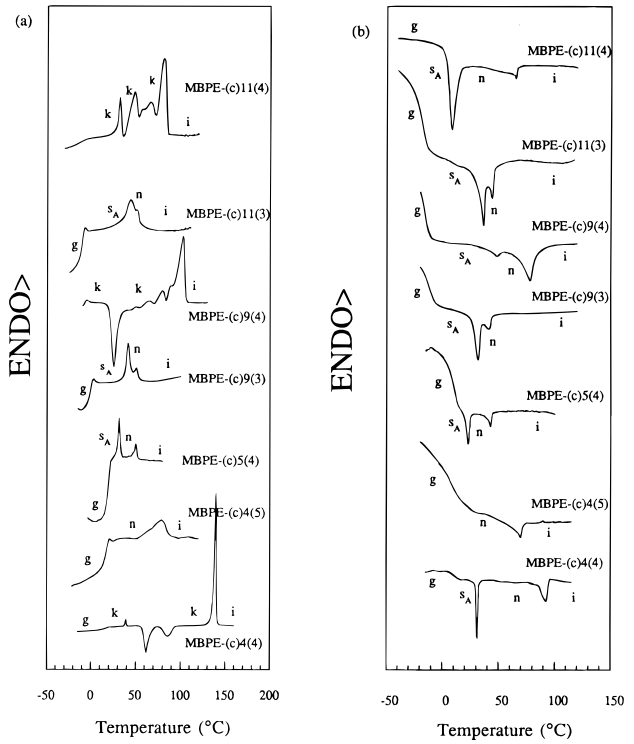

Figure 3. Selected DSC traces of the MBPE-(c)X(z) (X = 4, 5, 9, and 11 and z = 2−5) series: (a) second heating scan; (b) cooling scan.

of MBPE-(c)X(z). First, resonances corresponding to possible chain ends such as Ph−O*H*, −CH_2−Br, −CH_2−OH or −C*H*=CH_2 are absent. Second, the chemical shifts of most protonic resonances are strongly dependent on z, especially when z is small. This behavior is not observed for linear oligomers and is due to the ring-size-dependent conformations of the mesogen and spacer which translates into shielding and deshielding effects. At small z values or for short spacer lengths the mesogen is forced into the gauche conformation causing a downfield shift of all aromatic resonaces. A similar effect is observed for the aliphatic resonances, especially for the methylenic groups close to the ether linkage. With increasing X or z, as the ring strain alleviates, the population of the anti conformers of MBPE increases at the expense of the gauche ones, and eventually the trend reaches a plateau.

Selected DSC traces of MBPE-(c)X(z) are presented in Figure 3. The transition temperatures and the corresponding thermodynamic parameters for all cyclic compounds together with those of the corresponding linear polymers (MBPE-(l)X)[8b] are summarized in Table 1. The phase behavior of MBPE-(c)X(z) will be discussed first as a function of z at constant X, and then the spacer length (X) influence on the mesomorphic behavior of MBPE-(c)X(z) at constant z will be explained.

Figure 4a summarizes the phase behavior of MBPE-(c)4(z) and compares it to that of the linear polymer MBPE-(l)4.[8b] On the first heating scan, all MBPE-(c)4-(z) are crystalline and their melting temperatures follow an odd−even dependence on ring size. MBPE-(c)4(2) remains crystalline on subsequent cooling and heating scans, while MBPE-(c)4(3) is amorphous. MBPE-(c)4-(4) although crystalline on heating scans, on cooling dispays both smectic and nematic monotropic mesophases. MBPE-(c)4(5) is the only cyclic in this series displaying an enantiotropic nematic mesophase. The mixture of higher cyclic and linear oligomers as well as the corresponding linear polymer[8b] are only crystalline.

A similar phase behavior is observed for MBPE-(c)5-(z) (Figure 4b). Again, all MBPE-(c)5(z) are crystalline on their first heating scan. The dimer is crystalline, while the trimer is amorphous on both cooling and reheating. However, MBPE-(c)5(4) displays smectic A and nematic enantiotropic mesophases. The mixture of higher oligomers exhibits a monotropic nematic phase. The linear polymer MBPE-(l)5[8b] shows two monotropic nematic phases.

Figure 4c describes the phase behavior of MBPE-(c)9-(z). Even for longer spacers such as X = 9, on the first heating DSC scan the MBPE-(c)X(z) macrocyclics are crystalline. On further heating and cooling scans, the dimer remains crystalline, while the trimer dispays both nematic and smectic A enantiotropic mesophases. MBPE-(c)9(4) shows monotropic nematic and smectic A mesophases. The mixture of higher oligomers display a monotropic nematic mesophase. The linear polymer[8b] displays two monotropic nematic mesophases.

MBPE-(c)11(z) macrocyclics (Figure 4d) behave similar to MBPE-(c)9(z). On the first heating scan only a crystalline, melting is observed for all of them. MBPE-(c)11(2) is crystalline while MBPE-(c)11(3) displays enantiotropic nematic and smectic A phases. MBPE-(c)11(4) exhibits nematic and smectic A monotropic mesophases. The mixture of higher oligomers show a monotropic nematic phase. The corresponding linear polymer MBPE-(l)11 displays only a monotropic nematic phase. Its second nematic phase is virtual.[8b]

To explain the dependence of the phase behavior of MBPE-(c)X(z) on X, we must refer to their molecular conformation in their crystalline and LC phases.[2f,5] They are schematically shown in Figure 5. For short spacer lengths such as X = 4 and 5, the MBPE unit can not be accommodated in the cyclic monomer even in the gauche conformation. Therefore, MBPE-(c)X(1) with X = 4 and 5 do not form during the cyclization process. This was demonstrated by their absence in the reaction mixture. At longer spacers (X = 9 and 11) the gauche conformation of MBPE is still required in the ring closure of the monomer. This conformation however, cannot generate a collapsed rigid-rod-like structure; therefore, these cyclic monomers are only isotropic liquids. The most probable molecular arrangement of the dimers places the two MBPE mesogens in their anti conformation, symmetrically facing each other from opposite sides of the ring.[2f,5] This allows for a very economical crystalline packing and explains why MBPE-(c)X(2) are crystalline compounds. On increasing spacer length (Figure 6a), the melting temperature of the cyclic dimers decreases steadily.

Regardless of spacer length, on the first heating scan all MBPE-(c)X(3) are crystalline. As expected, on increasing spacer length, their glass transition temperature decreases. The phase behavior of the trimers on subsequent heating and cooling scans suggests two different classes of compounds. For cyclic trimers with short spacer lengths (X = 4 and 5) one of the mesogens should become part of the fold, and therefore this mesogen adopts a gauche conformation (Figure 6b).[2f] The collapsed shape of the resulting cyclic trimer is distorted. A rod-like supramolecular structure cannot

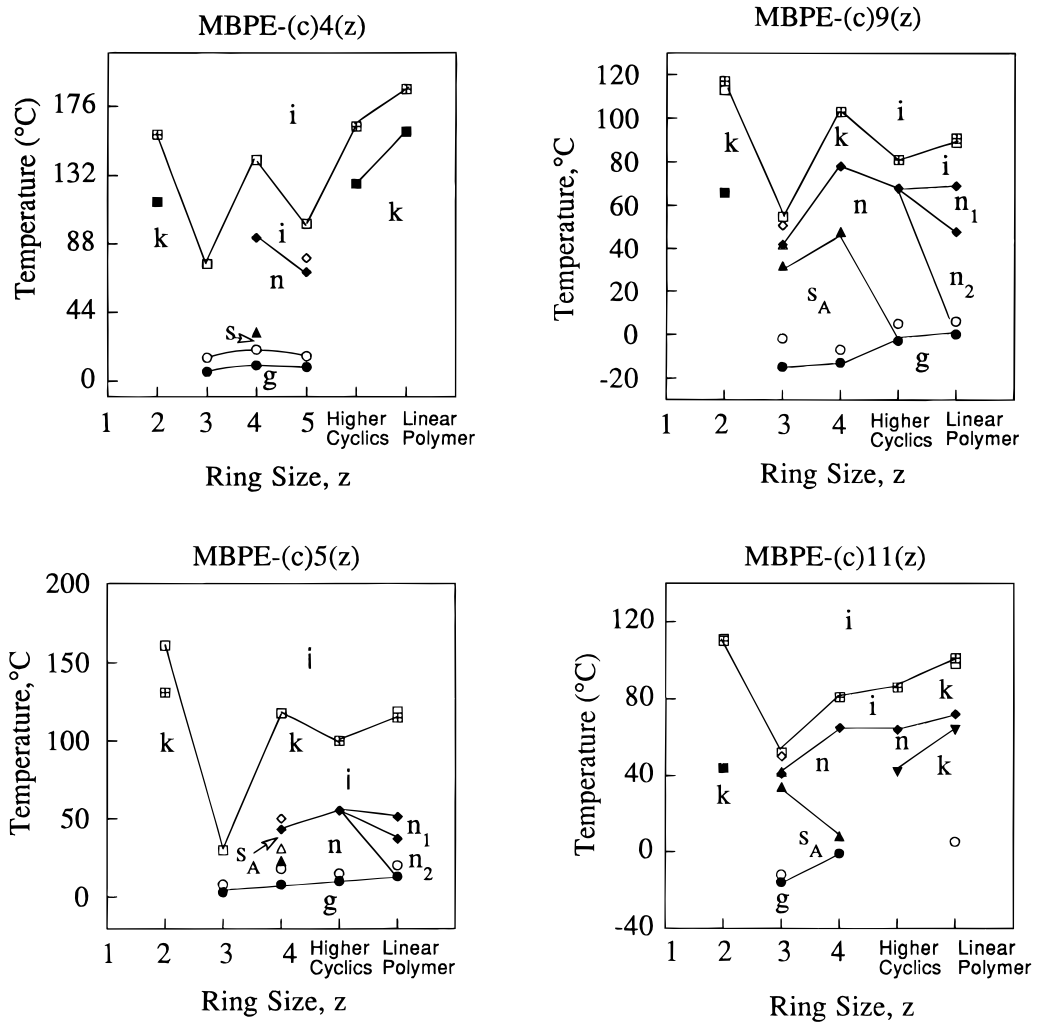

Figure 4. Dependence of the transition temperatures of the MBPE-(c)X(z) (X = 4, 5, 9, and 11 and z = 2−5) series on ring size and their comparison with the mixture of higher cyclics and with the corresponding linear polymer. Data collected from the first heating (T_{k-i} = □), first cooling (T_{i-k} = ■, T_{i-n} = ◆, T_{n-s} = ▲, T_{n-k} = ▼, T_g = ●) and second heating DSC scans (T_{k-i} = +, T_{n-i} = ◇, T_{s-n} = △, T_g = ○: (a, top left) MBPE-(c)4(z); (b, bottom left) MBPE-(c)5(z); (c, top right) MBPE-(c)9(z); (d, bottom right) MBPE-(c)11(z).

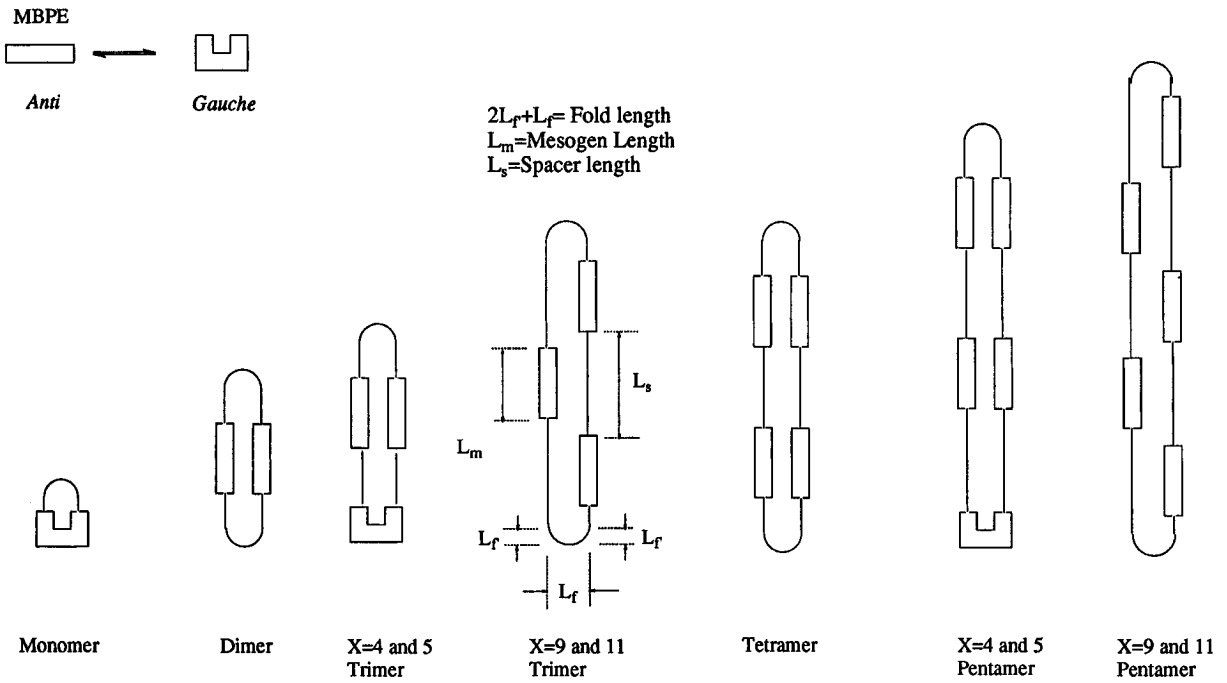

Figure 5. Molecular conformations of the cyclic oligomers in the crystalline or LC phases.

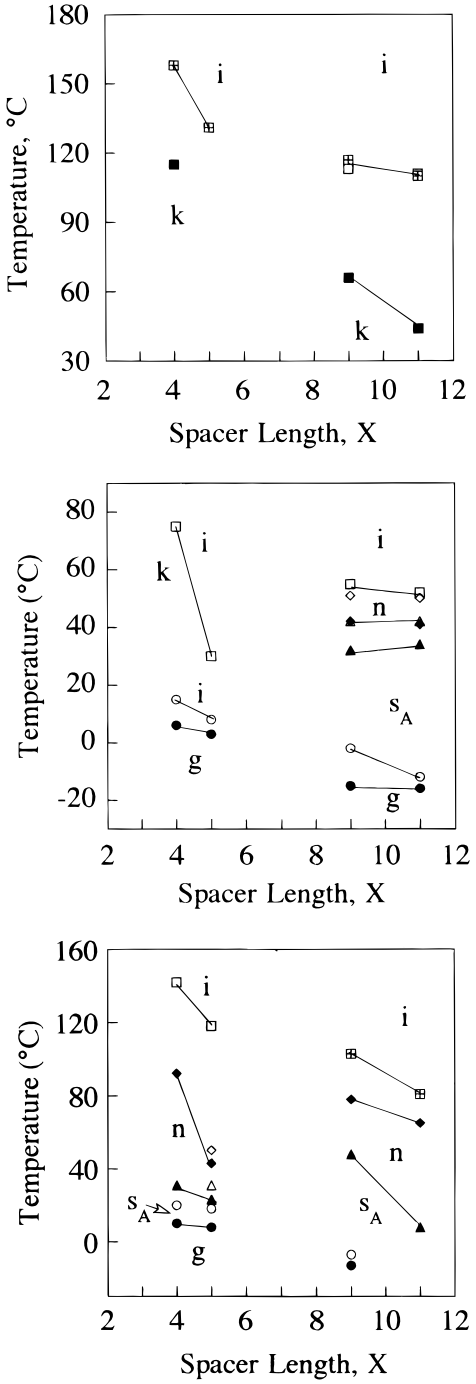

Figure 6. Dependence of the transition temperatures of MBPE-(c)$X(z)$ (X = 4, 5, 9, and 11 and z = 2−4) on spacer length (X). Data from the first heating (T_{k-i} = □), first cooling (T_{i-k} = ■, T_{i-n} = ◆, T_{n-s} = ▲, T_{n-k} = ▼, T_g = ●) and second heating DSC scans (T_{k-i} = +, T_{n-i} = ◇, T_{s-n} = △, T_g = ○): (a, top) MBPE-(c)X(2); (b, middle) MBPE-(c)X(3); (c, bottom) MBPE-(c)X(4).

be achieved by these cyclic trimers under these structural conditions and, therefore, both MBPE-(c)4(3) and MBPE-(c)5(3) are amorphous. When the spacer length is increased and the collapsed cyclic trimer exhibits a rodlike supramolecular structure all three MBPE units can addopt the anti conformation. This rodlike supramolecular structure should be able to generate LC phases and this is indeed the case since both MBPE-(c)9(3) and MBPE-(c)11(3) display enantiotropic nematic and smectic mesophases. The s_A phase of MBPE-(c)9-(3) was characterized by X-ray diffraction experiments.

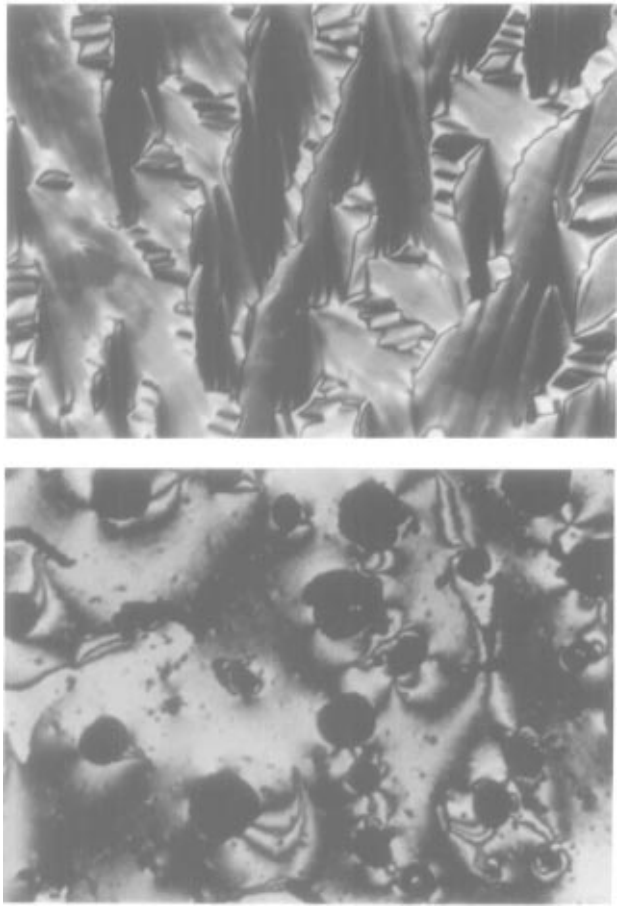

Figure 7. Representative optical polarized micrographs (×100) of (a, top) the s_A phase of MBPE-(c)9(3) after annealing at 39 °C for 2 h; (b, bottom) the nematic phase of MBPE-(c)5-(4) after annealing at 41 °C for 10 min.

The layer length of this phase is 34.1 Å. The length of the monomeric repeat unit (l_{ru}) containing one mesogen in its anti conformation and one flexible spacer with all the methylenic groups in the trans conformation can be estimated with the equation $l_{ru} = l_{MBPE} + 1.27X$, where l_{MBPE} = 12.5 Å, X is the number of methylenic units in the spacer, and 1.27 is the average contribution (Å) of each methylenic unit. For X = 9, l_{ru} = 23.9 Å. According to previous experiments,[2h] the calculated length of the collapsed strucure of MBPE-(c)9(3) is $L = 1.5l_{ru}$ = 35.9 Å. This value is in good agreement with the experimental value obtained by X-ray experiments and demonstrates that this phase is s_A. The s_A phase is formed by supramolecular rodlike groups obtained from collapsed macrocyclics in which extended combinations of anti MBPE and flexible spacers are linked by a sharp fold at each end. The minimum number of gauche methylenic units in the spacer required to achieve the 180° tight turn of the fold is two.[2h] This corresponds to 2.5 Å. A representative focal conic fan texture of the s_A phase of MBPE-(c)9(3) obtained at 39 °C is shown in Figure 7a.

Figure 6c summarizes the phase behavior of the cyclic tetramers. On their first DSC heating scan all MBPE-(c)X(4) are only crystalline. As expected, their melting temperature decreases continuously with increasing spacer length. The most probable structure (Figure 5) of MBPE-(c)X(4) in the crystaline or LC phase is the one in which each side of the collapsed macrocycle contains two MBPE groups in their anti conformation

separated by an extended spacer. The conformation of the macrocyclic tetramer allows for a good crystalline packing and for a better overall mesogenic character than the similar symmetric structure obtained from the cyclic dimers. All tetramers display both s_A and nematic monotropic phases. A notable exception is MBPE-(c)5-(4) for which both phases are enantiotropic. In this case the odd spacer helps to decrease the perfection of the crystalline phase just enough to uncover these mesophases also on the heating scan. A representative schlieren texture of the nematic phase of MBPE-(c)5-(4), obtained at 41 °C in shown in Figure 7b. The experimental value of the layer of the s_A phase of MBPE-(c)5(4) is 35.9 Å. The length of the monomeric repeat unit of MBPE-(c)5(4) is $l_{ru} = 12.5 + 1.27 \times 5 =$ 18.9 Å, and the calculated length of the collapsed supramolecular structure of this tetramer is $L = 2l_{ru} =$ 37.7 Å. A good agreement between the calculated and experimental values is observed.

At this point we will compare the phase behavior of MBPE-(c)*X*(*z*) with that of their linear homologues, MBPE-(l)*X*.[8] On the first and second heating, scans all linear polymers display only melting transitions. On the cooling scan, MBPE-(l)4 is crystalline while MBPE-(l)5, MBPE-(l)9, and MBPE-(l)11 exhibit monotropic nematic phases. The mesogenic character of these macrocyclics can be manipulated by changing both the spacer length and the ring size. In the field defined by these two variables there are points where a succesful combination of *X* and *z* leads to supramolecular rodlike macrocyclic mesogens with a higher ability to generate and stabilize LC phases than their corresponding linear structures.[2f,5] This is the case of MBPE-(c)4(5), MBPE-(c)5(4), MBPE-(c)9(3), and MBPE-(c)11(3). Therefore, virtual or monotropic LC phases of the linear polymers can be converted into monotropic or enantiotropic mesophases via cyclization.[2a,d] Moreover, it is also conceivable that even using a monomeric unit that would not lead to LC linear polymers, a suitable combination of *X* and *z* could still generate LC macrocyclics.

Both MBPE-(l)5 and MBPE-(l)9, which contain spacers with an odd number of methylenic units diplay two monotropic uniaxial nematic phases separated by a first-order phase transition.[8] This nematic−nematic transition was not detected in the corresponding macrocyclics. A speculative explanation for this behavior is as follows. According to Luckhurst's theoretical model,[9] only two conformers, *i.e.*, a linear one and a bent one, are sufficient to explain the phase behavior of LC polymers. When the mole fraction of the linear conformers in the isotropic phase is very small, two uniaxial nematic phases with different values of the order parameter may develop. This is the case for RBPE-(l)-*X* with *X* = odd and R = CH_3, CF_3, F, Cl, and Br.[8] The higher temperature nematic phase is less stable than the lower one since it still contains a large number of bent conformers. Due to the higher rigidity of the cyclic structure imparted by its collapsed topology,[4] the change in entropy as well as the change in the overall conformation at the isotropic−nematic transition is smaller for the cyclics than for their linear counterparts.[2h,5] This means that the difference between the number of extended conformers in the isotropic and nematic state is higher for the polymer than for the cyclic compounds. Since the linear polymers are almost fully extended[10] in the low-temperature range of their nematic phase, we can assume the same situation for the collapsed macrocyclics. This implies that there are more extended, collapsed, rodlike, cyclic conformers in the isotropic phase of the cyclics than are in the isotropic phase of the corresponding linear polymers. The collapsed macrocyclics contain at least two gauche methylenic units in each fold or a combination of a gauche mesogen and two *gauche* methylenic units.[2h] As a consequence, these collapsed structures tolerate much fewer conformers than their corresponding linear structures and most of them are rodlike. Therefore, the nematic phase generated from supramolecular collapsed macrocyclic rods contains a higher mole fraction of linear (in terms of Luckhurst's model[9]) conformers than the nematic phase of the corresponding linear structure. According to this model,[9] on cooling, only one nematic phase should form from collapsed macrocyclics.[9] Therefore, cyclic compounds are less likely to exhibit a second uniaxial nematic phase than are the linear structures. Nevertheless, when the s_A phase does not form, some collapsed macrocyclics are capable to generate a second nematic phase which is biaxial.[3] These results provide additional examples of molecular engineering of the phase behavior of macrocyclic liquid crystals by learning from the differences and similarities between macrocyclic and linear compounds.

Acknowledgment. Financial support by the National Science Foundation (DMR-92-06781 and DMR-91-22227) is gratefully acknowledged.

CM9602048